Scientific Research Publishing

Open Journal of Applied Sciences, 2022, 12, 1749-1757
https://www.scirp.org/journal/ojapps
ISSN Online: 2165-3925
ISSN Print: 2165-3917

Contribution of the International Reference Ionosphere-2016 Model in the Evidence of the Winter Anomaly

Moustapha Konaté[1,2*], Raoul Ilboudo[1], Kadidia Nonlo Drabo[1], Emmanuel Nanéma[1,3], Frédéric Ouattara[1]

[1]Unité de Recherche et de Formation en Sciences et Technologie (UFR-ST), Laboratoire de Recherche en Energétique et Météorologie de l'Espace (LAREME), Université Norbert Zongo, Koudougou, Burkina Faso
[2]Centre Universitaire de Gaoua, Université Nazi BONI, Bobo Dioulasso, Burkina Faso
[3]Centre National de la Recherche Scientifique et Technologique (CNRST), Institut de Recherche en Sciences Appliquées et Technologies (IRSAT), Ouagadougou, Burkina Faso
Email: *konat_moustapha@yahoo.fr

How to cite this paper: Konaté, M., Ilboudo, R., Drabo, K.N., Nanéma, E. and Ouattara, F. (2022) Contribution of the International Reference Ionosphere-2016 Model in the Evidence of the Winter Anomaly. *Open Journal of Applied Sciences*, **12**, 1749-1757.
https://doi.org/10.4236/ojapps.2022.1211120

Received: September 28, 2022
Accepted: November 4, 2022
Published: November 7, 2022

Abstract

This study is a contribution to the estimation of the winter anomaly in the F2 layer of the ionosphere at low latitudes. The aim is to study the variability of the virtual height (hmF2) of the F2 region of the ionosphere through the predictions of the latest International Reference Ionosphere model (IRI-2016). The present work allows analyzing the temporal evolution of hmF2 according to the different phases of three (3) solar cycles during the quiet geomagnetic activity to estimate the seasonal anomaly at the Ouagadougou station. The analysis of the seasonal profiles shows that the variability of hmF2 is: 1) strongly linked to the solar cycle activity, 2) dependent on the season and 3) variable from one cycle to the next for the same phase. It appears that hmF2 increases during the ascending phase to reach its maximum value at the phase maximum. During the descending phase, it decreases until the phase minimum where it finds its minimum value. The difference between winter and summer on the hmF2 values for each phase of the cycle is obtained at the phase minimum and is estimated to be at least 16 km. In low latitudes, solar irradiation is greater in summer than in winter. From this study, hmF2 values are larger in winter compared to summer indicating an anomaly in the virtual height of the F2 layer of the ionosphere through the predictions of IRI-2016 at the Ouagadougou station.

Keywords

Winter Anomaly, IRI, hmF2, Quiet Day, Solar Cycle Phases

1. Introduction

The ionosphere is the part of the Earth's atmosphere where high-energy solar radiation causes the ionization of the particles present in this zone [1]. This layer, because of its particle composition and its location, is important for navigation and satellite communication. Many models exist to study the dynamics of the ionospheric layer [2] [3] [4]. Some are based mainly on purely mathematical models, others on the other hand, on *in situ* measurements recorded on the various stations. These models allow either to validate dynamo theories [5], or to reproduce the characteristics of the ionosphere [6] [7]. The International Reference Ionosphere (IRI) model is a semi-empirical model which allows reproducing the characteristic parameters of the ionosphere. Numerous studies have been conducted to understand the morphology of the variation of ionospheric parameters especially in low latitudes as a function of the model, solar cycles, solar cycle phases, seasons and the impact of different classes of geomagnetic activities [8] [9] [10] [11] through various data sources. The present study focuses on the IRI-2016 predictions on the virtual height parameter of the F2 layer of the ionosphere (hmF2) to analyze the seasonal variation at the Ouagadougou station (Latitude 12.5˚N and Longitude 358.5˚E) during the different phases of the solar cycle C21, C22 and C23. The objective is to compare the height of this layer between summer, which is a period characterized by high solar irradiation, and winter by low sunshine at low altitudes. It allows to contribute to the estimation of the seasonal anomaly in low latitudes, whose phenomenon has been studied by the authors [12] [13] [14] through different parameters and ionospheric data sources.

2. Materials and Methods

The methodology of this study on the variation of seasonal mean values is based on the following assumptions: 1) the quiet day is determined by the index $Aa \leq 20$ nT [15]; 2) the season is characterized by its characteristic month namely: March for spring, June for summer, September for autumn, and December for winter [16]; and 3) the phases of the solar cycle are determined by the annual average of the number of spots (or Wolf number) *Rz*. For the minimum phase $Rz < 20$, the rising and falling phase $20 < Rz < 100$ and the maximum phase $Rz > 100$ [17]. From one maximum to the next, the solar cycle lasts on average 11 years and is related to the activity of spot cycle [18]. The solar cycles 21, 22 and 23 last respectively: 1976-1985, 1985-1996 and 1996-2006. The study of the variation of the average ionospheric values [19] is carried out according to the four phases of the solar cycle (minimum, ascending, maximum and descending) [20]. From this subdivision of the solar cycle, we can determine the years that belong to each phase of the three (3) solar cycles studied. The quietest day describes the whole season and the Ouagadougou station is determined by the geographical coordinates: latitude 12.4˚N and longitude 358.5˚E. The IRI model is run under conditions (1), (2) and (3) to determine the hourly average values of

the virtual height. The data is then exported to an Excel file for the calculation of mean values, variation and curve plots. Equation (1) gives the seasonal average value of the virtual height.

$$hmF2_{mean} = \frac{\sum_{h=0}^{i} hmF2_{j,d}}{i} \quad (1)$$

In this equation, $hmF2_{mean}$ denotes the seasonal mean value of $hmF2$ of the considered characteristic month of the season; $hmF2_{j,h}$ is the hourly mean value of the virtual height at time h for day d. Under these conditions, the index $h \in [0, 24]$, the index $d \in [1, 31]$, and $i = 25$. Equation (2) is used to calculate the annual average value of the solar cycle phase.

$$hmF2_{mean.ann} = \frac{\sum_{s=0}^{n} hmF2_{mean}}{n} \quad (2)$$

From Equation (2), $hmF2_{mean.ann}$ denotes the annual average value of the minimum, rising, maximum or falling phase of hmF2 and n the number of years of the phase considered.

Equation (3) allows us to estimate the variation of hmF2 between winter and summer for the different phases

$$\Delta hmF2_{mean.ann} = hmF2_{mean.ann}(winter) - hmF2_{mean.ann}(summer) \quad (3)$$

In this equation, $\Delta hmF2_{mean.ann}$ is the change in height between winter and summer for a given phase. $hmF2_{mean.ann}(winter)$ and $hmF2_{mean.ann}(summer)$ are the mean hmF2 values in winter and summer.

Equation (4) estimates the change in virtual height between winter and summer as a function of the percentage of hmF2 in winter.

$$\%P_{hmF2(winter)} = \frac{\Delta hmF2_{mean.ann}}{hmF2_{mean.ann}(winter)} \times 100 \quad (4)$$

$\%P_{hmF2(winter)}$: Percentage difference between winter and summer expressed as a function of hmF2 in winter.

3. Results and Discussion

Using assumption (2), June defines summer and December defines winter. According to the principle (3) for the solar cycle: solar cycle 21: the minimum phase is 1976, the ascending phase goes from 1977 to 1979, the maximum phase is 1980 and the descending phase goes from 1981 to 1984; solar cycle 22: the minimum phase is 1985, the ascending phase goes from 1986 to 1989, the maximum phase is 1990 and the descending phase goes from 1991 to 1995 for the solar cycle; solar cycle 23: the minimum phase is 1996, the ascending phase goes from 1997 to 2000, the maximum phase is 2001 and the descending phase goes from 2002 to 2005.

Table 1 is obtained using conditions (1), (2), and (3). It shows the quietest day of summer and winter during the different phases of solar cycles 21, 22 and 23.

For each characteristic day of the season, the IRI model is run under conditions

Table 1. Distribution of the quietest days during the phases of solar cycles 21, 22 and 23.

Phase	Solar cycle 21			Solar cycle 22			Solar cycle 23		
	Year	Winter	Summer	Year	Winter	Summer	Year	Winter	Summer
Minimum	1976	14	15	1985	16	21	1996	13	19
Increasing	1977	11	8	1986	25	29	1997	21	8
	1978	9	10	1987	30	8	1998	14	17
	1979	28	7	1988	4	7	1999	14	26
				1989	18	10	2000	16	31
Maximum	1980	17	24	1990	20	10	2001	28	9
Decreasing	1981	12	6	1991	29	6	2002	1	17
	1982	17	1	1992	4	26	2003	12	19
	1983	4	9	1993	21	9	2004	22	4
	1984	21	24	1994	23	22	2005	21	7
				1995	12	13			

(1) for the determination of hmF2 and the use of Equation 1 generates the daily average value of hmF2 during the characteristic year of the cycle phase ($hmF2_{mean}$). The annual average virtual height values ($hmF2_{mean.ann}$) are obtained using Equation (2) during the phases.

Figures 1-3 represent the variation of hmF2 during the phases of solar cycles 21, 22 and 23 in summer and winter. This study takes into account the different phases of the solar cycle and allows us to analyze the evolution of the virtual heights. From the right to the left, we have the minimum phase, the rising phase, the maximum phase, the falling phase and the minimum phase of the next cycle.

Figure 1 shows the evolution of hmF2 during the summer and winter phases of solar cycle 21. The analysis of this figure shows that hmF2 is related to the solar cycle activity. The height shows minimum values at the phase minimum namely 327 km for winter and 310 km for summer. During the rising phase, hmF2 increases to reach its maximum value at 467 km for winter and 405 km for summer at the phase maximum. Then, it decreases during the descending phase until the next phase minimum. The difference between the maximum and minimum value during cycle 21 and for the same season is 140 km for winter and 95 km for summer. Examination of the figure also indicates that there is a remarkable seasonal variation between winter and summer in hmF2. For all phases of cycle 21, the virtual height in summer is lower than in winter. The variation in virtual height between the two seasons is estimated to be: 17.02 km (5.20% winter hmF2), 58.41 km (13.92% winter hmF2), 62.43 km (13.35% winter hmF2), and 22.28 km (5.74% winter hmF2) for phases: minimum, rising, maximum, and falling, respectively.

The seasonal variations of hmF2 in summer and winter for the solar cycle 22

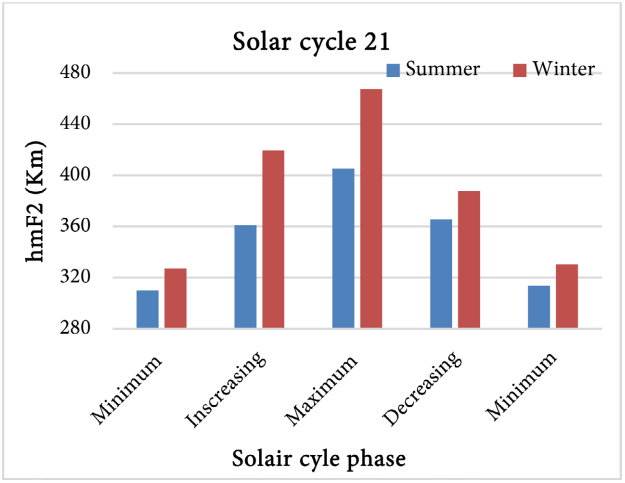

Figure 1. Variation of hmF2 in summer and winter according to solar cycle phases 21.

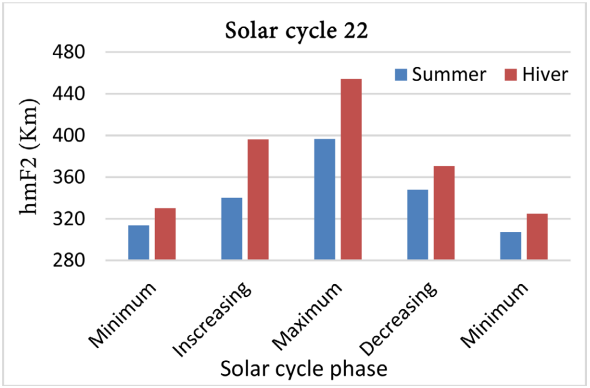

Figure 2. Variation of hmF2 in summer and winter according to solar cycle phases 22.

phases are given in Figure 2. The morphological analysis of Figure 2 shows that hmF2 is also related to solar cycle activity. For this figure, hmF2 also has minimum values at the phase minimum at 330 km for winter and 313 km for summer. The virtual height increases during the rising phase to reach its maximum value at the phase maximum at 454 km for winter and 396 km for summer and decreases during the falling phase to the next phase minimum. The difference between the maximum and minimum value is estimated at 164 km for winter and 83 km for summer. Figure 2 shows a seasonal variation on the hmF2 parameter. During the phases of cycle 22, hmF2 in summer is lower than in winter. The variation in virtual height between the two seasons for cycle 22 is estimated to be: 16.52 km (5.00% of hmF2 in winter); 56.03 km (14.14% of hmF2 in winter); 57.39 km (12.63% of hmF2 in winter) and 22.73 km (6.13% of hmF2 in winter) for the phases: minimum, rising, maximum and falling, respectively.

Figure 3 shows the evolution of hmF2 during the summer and winter phases of solar cycle 23. The examination of Figure 3 is identical to that of Figure 1 and Figure 2. The minimum values of hmF2 during the phase minimum are obtained at 324 km for winter and 307 km for summer. At the phase maximum, the values of hmF2 are 424 km for winter and 373 km for summer. The difference

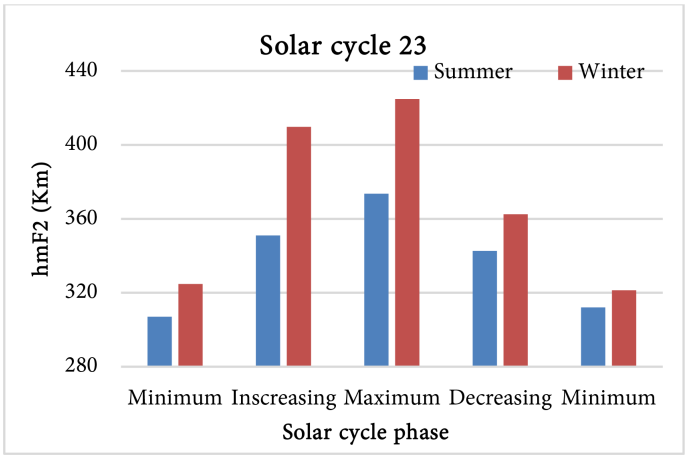

Figure 3. Variation of hmF2 in summer and winter as a function of solar cycle phases 23.

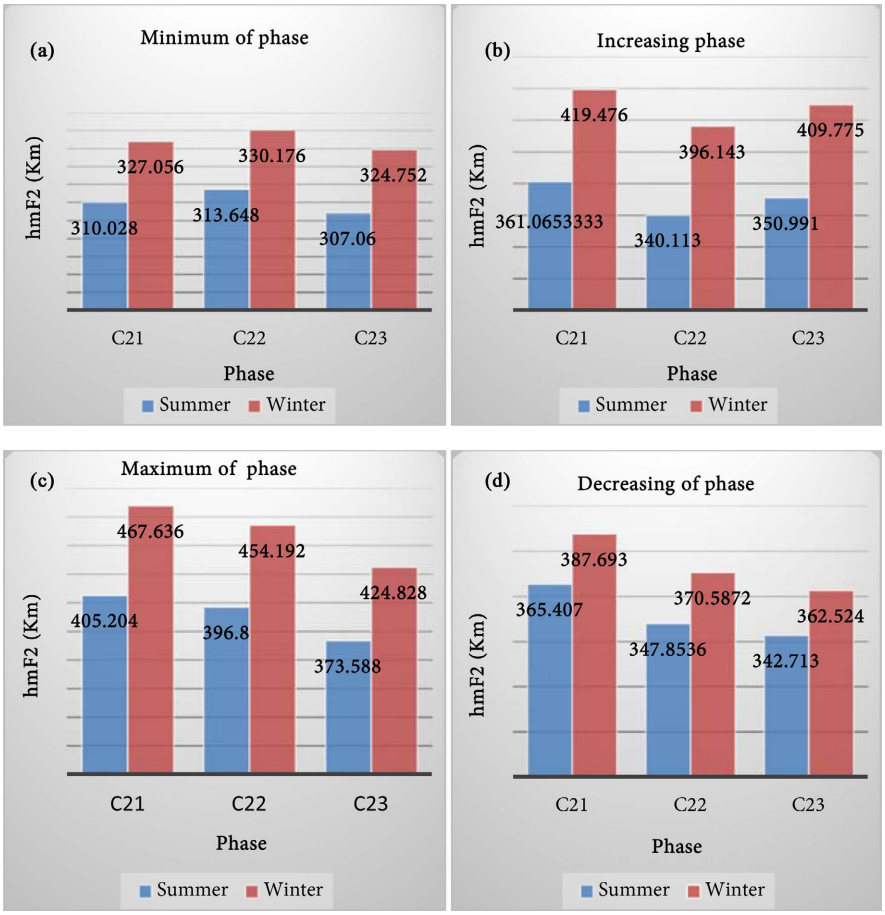

Figure 4. Variation of hmF2 in summer and winter as a function of the phases of solar cycles 21, 22 and 23. (a) Variation of hmF2 at the phase minimum of solar cycles 21, 22 and 23. (b) Variation of hmF2 during the increasing phases of solar cycles 21, 22 and 23. (c) Variation of hmF2 at the maximum of the phases of solar cycles 21, 22 and 23. (d) Variation of hmF2 during the decreasing phases of solar cycles 21, 22 and 23.

between the maximum and minimum value during solar cycle 23 and for the same season is 100 km for winter and 66 km for summer. The graphical analysis

in Figure 3 shows that there is a seasonal variation on the mean values of hmF2 between winter and summer. For all phases of cycle 23, it is noticed that hmF2 in summer is lower than in winter. The variation in height between the two seasons is estimated to be about 17.69 km (5.44% of hmF2 in winter) for the minimum phase; 58.78 km (14.34% of hmF2 in winter) for the rising phase; 51.24 km (12.06% of hmF2) for the phase maximum and 19.81 km (5.46% of hmF2 in winter) for the falling phase.

Figure 4 shows the seasonal variation of hmF2 for quiet geomagnetic activity during the phase minimum (Figure 4(a)), the rising phase (Figure 4(b)), the phase maximum (Figure 4(c)) and the falling phase (Figure 4(d)) of solar cycles 21, 22, 23 at the Ouagadougou station.

The analysis of Figure 4 shows that the parameter hmF2 depends on the phase of the solar cycle. During the ascending phase, the phase maximum and the descending phase of the solar cycle, the height of the F2 region of the ionosphere presents values whose minimum is above 340 km. On the other hand, during the phase minimum, the values of hmF2 are below 340 km. Thus, during a phase maximum, the height of the F2 region of the ionosphere is higher than during other phases of the solar cycle. Moreover, for the same phase, the hmF2 profiles vary from one cycle to the next. The hmF2 profiles in winter for each phase of the cycle are higher than those in summer during the three (3) cycles studied. The percentage of winter hmF2 obtained for the different phases is at least: 5%, 13.92%, 12.06% and 5.46% for the phase minimum, rising phase, phase maximum and falling phase respectively. The anomaly is more accentuated during the ascending and maximum phases.

4. Conclusion

This study makes a comparison of the height of the F2 region of the ionosphere in summer and winter during periods of quiet geomagnetic activity in low latitudes using the IRI-2016 model. The study presented hmF2 profiles in summer and winter during solar cycles 21, 22 and 23 at the Ouagadougou station. The analysis of seasonal profiles of hmF2 variability during the three solar cycles shows that hmF2 is strongly related to the solar cycle activity and varies from one cycle to the next. Similarly, examination of the profiles indicates variations as a function of the solar cycle phase. Maximum and minimum values are obtained respectively during the maximum and minimum of the solar cycle phase. Also, for the same phase, the profiles vary from one cycle to the next. The influence of the season on the height of the F2 region of the ionosphere is highlighted. The values of hmF2 in winter for each phase of the cycle are 16 km higher (5% of hmF2 in winter) than those in summer during the three (3) cycles studied. The solar radiation intensity is higher in low latitudes in summer compared to other seasons of the year and especially in winter. From this study, the electron production process is more important in winter creating a higher virtual height than in summer. This work highlights the winter anomaly in the virtual height parameter and shows that the phenomenon is more accentuated during the as-

cending and maximum phases for solar cycles 21, 22 and 23 through the predictions of IRI-2016.

Acknowledgements

The authors thank the International Reference Ionosphere model for making the data available and express their appreciation to the journal for publishing the article.

Conflicts of Interest

The authors declare no conflicts of interest regarding the publication of this paper.

References

[1] Rishbeth, H. and Garriott, O.K. (1969) Introduction to Ionospheric Physics. International Geophysics Series. Academic Press, New York, 120-121.

[2] Bilitza, D., Altadill, D., Zang, Y., Mertens, C., Truhlik, V. and Richards, P. (2014) The International Reference Ionophere 2012—A Model of International Collaboration. *Journal of Space Weather and Space Climate*, **4**, Article No. A07. https://doi.org/10.1051/swsc/2014004

[3] Qian, L., Burns, A.G., Chamberlin, P.C. and Solomon, S.C. (2010) Flare Location on the Solar Disk: Modeling the Thermosphere and Ionosphere Response. *Journal of Geophysical Research*, **115**, Article No. A09311. https://doi.org/10.1029/2009JA015225

[4] Richmond, A.D., Ridley, E.C. and Roble, R.G. (1992) A Thermosphere/Ionosphere General Circulation Model with Coupled Electrodynamics. *Geophysics Research Letters*, **19**, 601-604. https://doi.org/10.1029/92GL00401

[5] Schunk, R.W. (1996) Handbook of Ionospheric Models, Chap. A Coupled Thermosphere-Ionosphere Model (CTIM). Utah State University, Logan, Utah, 217-238.

[6] Anderson, D.N., Mendillo, M. and Herniter, B. (1987) A Semi-Empirical, Low-Latitude Ionospheric Model. *Radio Science*, **22**, 292-306. https://doi.org/10.1029/RS022i002p00292

[7] Daniell Jr., R.E., Brown, L.D., Anderson, D., Fox, M.W., Doherty, P.H., Decker, D.T., Sojka, J.J. and Schunk, R.W. (1995) Parameterized Ionospheric Model: A Global Ionospheric Parameterization Based on First Principles Models. *Radio Science*, **30**, 1499-1510. https://doi.org/10.1029/95RS01826

[8] Ouattara, F., Amory-Mazaudier, C. (2008) Solar-Geomagnetic Activity and Aa Indices toward a Standard. *Journal of Atmospheric and Solar-Terrestrial Physics*, **71**, 1736-1748. https://doi.org/10.1016/j.jastp.2008.05.001

[9] Ouattara, F. and Nanéma, E. (2014) Quiet Time foF2 Variation at Ouagadougou Station and Comparison with TIEGCM and IRI-2012 Predictions for 1985 and 1990. *Physical Science International Journal*, **4**, 892-902. https://doi.org/10.9734/PSIJ/2014/9748

[10] Nanéma, E., Gnabahou, D.A., Zoundi, C. and Ouattara, F. (2018) Modeling the Ionosphere during Quiet Time Variation at Ouagadougou in West Africa. *International Journal of Astronomy and Astrophysics*, **8**, 163-170. https://doi.org/10.4236/ijaa.2018.82011

[11] Konaté, M., Nanéma, E. and Ouattara, F. (2019) Variabilité du pic de la densité des électrons dans l'ionosphère au maximum de phase du cycle solaire. *Sciences Na-*

turelles et Appliquées, **38**, 93-100.

[12] Rishbeth, H., Muller-Wodarg, I.C.F., Zou, L., Fuller-Rowell, T.J., Millward, G.H., Moffett, R.J., Idenden, D.W. and Aylward, A.D. (2000) Annual and Semiannual Variations in the Ionospheric F2-Layer: II. Physical Discussion. *Annales Geophysicae*, **18**, 945-956. https://doi.org/10.1007/s00585-000-0945-6

[13] Rishbeth, H. and Muller-Wodarg, I.C.F. (2006) Why Is There More Ionosphere in January than in July? The Annual Asymmetry in the F2-Layer. *Annales Geophysicae*, **24**, 3293-3311. https://doi.org/10.5194/angeo-24-3293-2006

[14] Nanéma, E., Konaté, M., Zoundi, C., Kotia, A.O., Zerbo, J.L. and Ouattara, F. (2021) Evaluating the Rate of Total Electron Content (TEC) Production in Ionosphere F2-Layer to Highlight Winter Anomaly by Running Thermosphere-Ionosphere-Electrodynamics General Circulation Model. *African Journal of Environmental Science and Technology*, **15**, 379-383. https://doi.org/10.5897/AJEST2021.3051

[15] Nanéma, E., Konaté, M. and Ouattara, F. (2019) Peak of Electron Density in F2-Layer Parameters Variability at Quiet Days on Solar Minimum. *Journal of Modern Physics*, **10**, 302-309. https://doi.org/10.4236/jmp.2019.103021

[16] Gnabahou, A. and Ouattara, F. (2012) Ionosphere Variability from 1957 to 1981 at Djibouti Station. *European Journal of Scientific Research*, **73**, 382-390.

[17] Ouattara, F., Zoundi, C. and Fleury, R. (2012) Comparison between CODG TEC and GPS Based TEC Observations at Koudougou Station in Burkina Faso. *Indian Journal of Radio and Space Physics*, **41**, 617-623. https://hal.archives-ouvertes.fr/hal-00940398

[18] Zerbo, J.L., Ouattara, F., Zoundi, C. and Gyébré, A. (2011) Solar Cycle 23 and Geomagnetic Activity since 1868. *Revue CAMES Série A*, **12**, 255-262.

[19] Rishbeth, H. and Mendillo, M. (2001) Patterns of F2 Layer Variability. *Journal of Atmospheric and Solar Terrestrial Physics*, **63**, 1661-1680. https://doi.org/10.1016/S1364-6826(01)00036-0

[20] Ouattara, F., Amory-Mazaudier, C., Menvielle, M., Simon, P. and Legrand, J.-P. (2009) On the Long Term Change in the Geomagnetic Activity during the 20th Century. *Annales Geophysicae*, **27**, 2045-2051. https://doi.org/10.5194/angeo-27-2045-2009